# Satellite Signatures in SLR Observations

G.M. Appleby
Royal Greenwich Observatory
Madingley Road
Cambridge CB3 0EZ, UK

## Abstract.

*We examine the evidence for the detection of satellite-dependent signatures in the laser range observations obtained by the UK single-photon SLR system. Models of the expected observation distributions from Ajisai and Lageos are developed from the published satellite spread functions and from the characteristics of the SLR system, and compared with the observations. The effects of varying return strengths are discused using the models and by experimental observations of Ajisai, during which a range of return levels from single to multiple-photons is achieved. The implications of these results for system-dependent centre of mass corrections are discussed.*

## 1. Introduction.

The UK SLR system sited at Herstmonceux, and run by the Royal Greenwich Observatory, routinely observes the primary targets ERS-1, Lageos, Etalon-1 and -2, Starlette and Ajisai. The single-shot precision achieved by calibration ranging is close to 1 cm (1-sigma). The detection and timing hardware has recently been upgraded to include a Single Photon Avalanche Photodiode (SPAD, Prochazka et al, 1990), and an HP 5370 time interval counter. Epoch is derived at present from a Maryland 4-stop event timer, which is also used to make range measurements simultaneously and independently of the HP counter. Pass-averaged return rates are in general fairly low, varying from a few percent from the Etalon satellites, through about 20% from Lageos to up to 50% from Ajisai. Returns from the calibration targets are deliberately kept to similarly low levels (about 10-15%) using neutral density filters in the laser path. Under such conditions we can describe the system as a single photon return, single photon detection system. A detailed study of the system error budget was carried out following the upgrade of the detector from a PMT. During this investigation it became clear that the observational precision of in particular Lageos and Ajisai was consistently worse than that of the calibration targets. It was considered likely that the spacial distribution of the retroreflector arrays on the satellites would modify the distribution of the range residuals, when compared with those from the flat calibration targets. In this paper we examine the evidence for detection of satellite signatures in our range observations, compare the observations with models of the expected distributions from a selection of those satellites regularly observed, and discuss the implications in terms of the appropriate corrections required to reduce the observations to the centres of mass of the satellites

## 2. Observations.

This investigation is based upon the pass-by-pass range residuals that are formed during

the preprocessing stage to compute on-site normal points. All trends in the residuals due to errors in the predicted orbit of the satellite are removed during this process, which iteratively solves for corrections to a set of orbit-related parameters, rejecting at each stage residuals falling outside a 3-sigma band (Appleby and Sinclair, 1992, these proceedings). In a final stage of pre-processing, and as a useful check on system performance, the residuals are used to form a frequency distribution for each pass, by grouping the residuals in range bins. A normal distribution is fitted to the observed distribution by iterative least-squares, and the parameters of the fitted Gaussian are used to make a final selection of the original observations. Examples of the observed distributions and their fitted Gaussian distributions are shown in Figure 1. Also shown in the Figure is a typical distribution of ranges to a calibration target board, distant about 600 m from the SLR system. The observed range values are plotted relative to the mean of the fitted Gaussian distributions, which are also shown on each plot. The standard deviations of the fitted distributions are shown, along with higher moments of the data, expressed as skewness and kurtosis. For a perfect Gaussian distribution the values of skewness and kurtosis would be 0.0 and 3.0 respectively.

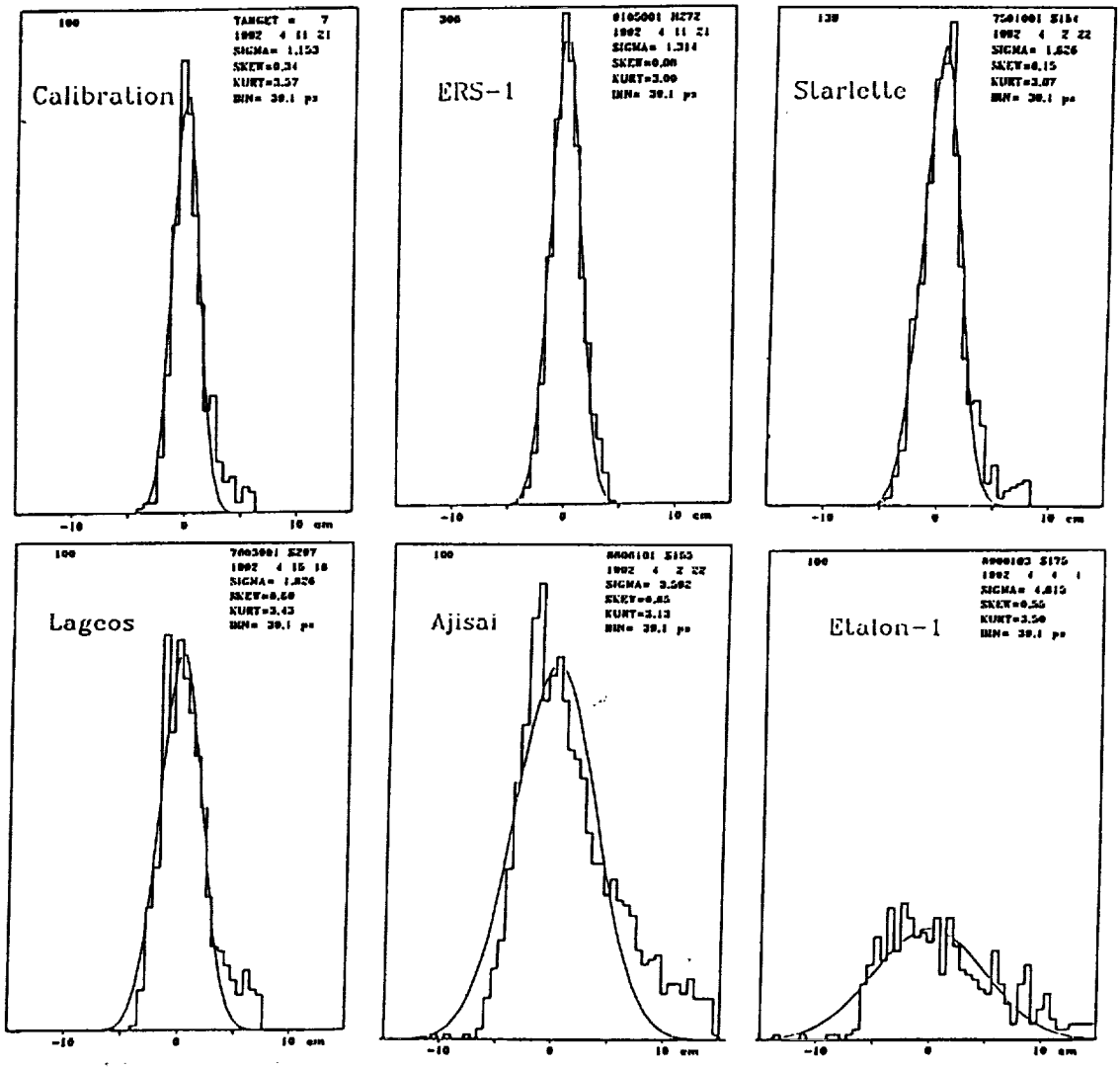


Figure 1. Observed distributions of range residuals from calibration and satellite targets.

### 2.1 Discussion.

From the distributions shown in Figure 1, we make the following observations. The distributions of the calibration ranges and those from Starlette and ERS-1 are clearly symmetric and well-fitted by the Gaussian distributions, but all have a significant 'tail' of observations outside the fitted curves. Skewness values for these 3 targets are between 0.05 and 0.1. The Lageos distribution is much less symmetric, and is less well fit by the Gaussian distribution. A chi-square goodness of fit test indicates significant departure, at a 5% level of significance, from the best-fit distribution shown in the plot. The results from Ajisai and Etalon 1 show large asymmetry, and are not at all well fit by the Gaussian distributions. Of particular significance to this investigation, are the 'widths' of the distributions, characterized by the standard deviations of the fitted distributions. Mean values of these standard deviations for a number of observations made during November and December 1991 are given in the Table below. These mean values of standard deviations confirm the impression given in Figure 1, that the calibration ranges have the smallest scatter, and those of Ajisai and Etalon-1 the largest, the range of standard deviations being from 1.1 cm to 4.8 cm.

| Target | $\sigma$ |
|---|---|
| | mm |
| Calib | 11 |
| ERS-1 | 12 |
| Starlette | 16 |
| LAGEOS | 18 |
| Ajisai | 32 |
| Etalon | 48 |

Before proceeding to investigate the hypothesis that satellite signatures are present in our observations, we first consider the possible causes of the 'tail' in the distributions, particularly evident in the calibration and Starlette data. We remark here that the existence of this tail does not constitute the thrust of our argument that we are detecting satellite signatures in our observations, since the tail is also present in the calibration ranges from a flat target board. We must therefore rule out such a target-induced effect and consider as probable cause the SPAD or the laser. In an experiment primarily designed to quantify the system time-walk under a large range of return signal strengths, calibration ranging was carried out using neutral density filters to vary the average number of photons reaching the detector. In this way the average number of photons was varied from about 0.5 to 50 photons per shot, as deduced from the observed return rates. A selection of the results is given in Figure 2, where the results are displayed in histogram form as before. The plots show, as expected, a reduction in the standard deviations of the distributions with increasing signal strength, since for a given laser pulse-width we would expect the contribution of the laser to the observational jitter to decrease with increasing number of photons in the return train, as the single-event detector increasingly receives photons originating nearer to the leading edge of the transmitted pulse. The plots also demonstrate that the extent of the tail in the distributions decreases with signal strength, suggesting an origin within the laser. However Prochazka (1992, private communication), points out that correct optical alignment

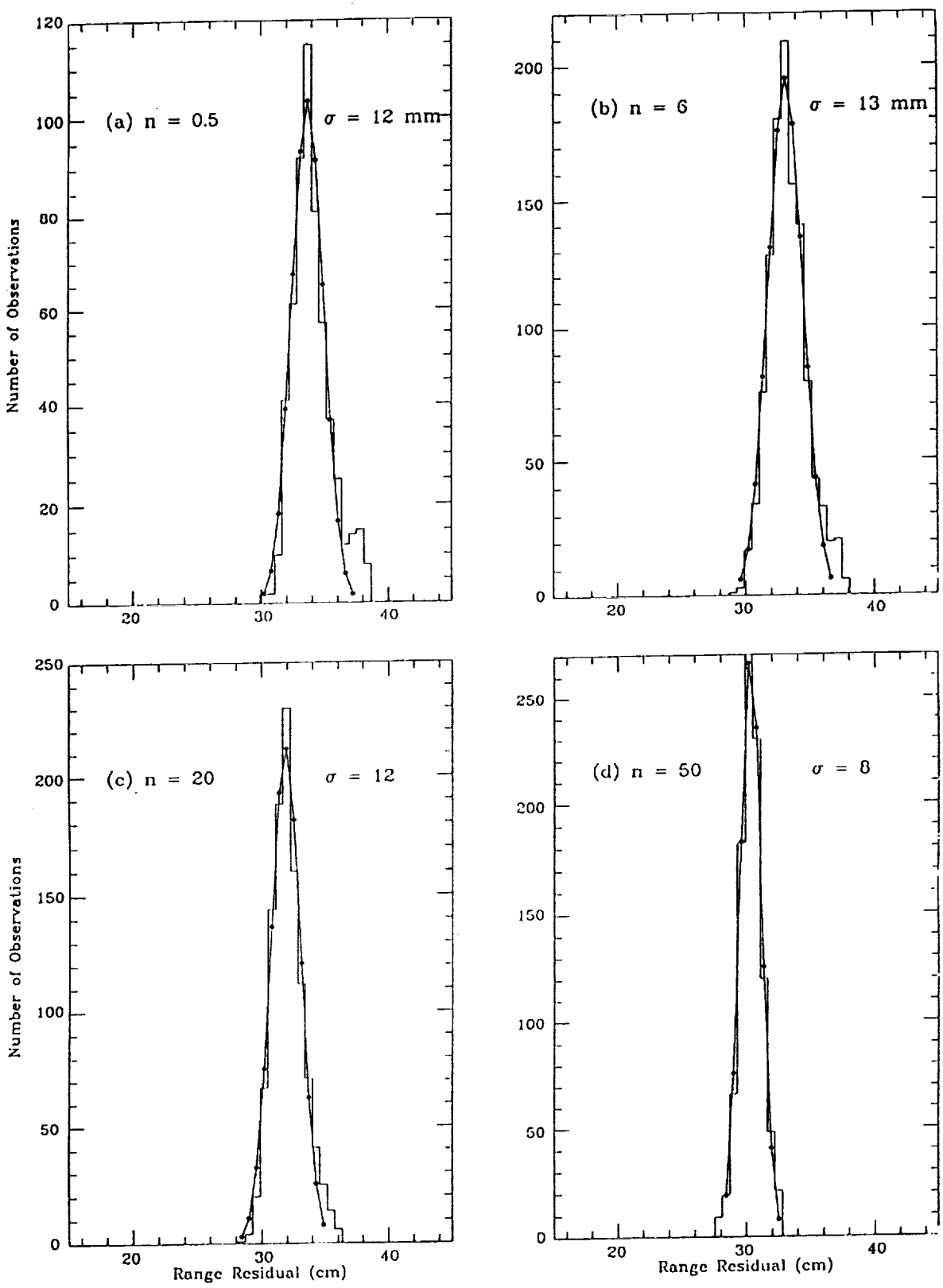


Figure 2. Calibration distributions as a function of average numbers $n$ of returning photons.

of the SPAD detector is essential to avoid possible effects of non-uniformity within the chip. Resolution of this problem awaits further experimentation.

## 3. Satellite Signature Models.

We now take as our standard, single-photon system-signature the calibration distribution shown in Figure 1, and develop from it models of expected satellite return signatures, by convolution with the spread functions of Lageos and Ajisai. For Lageos, we take the model of cross-section parameters based upon row-by-row far-field diffraction pattern tests in polar orientation, presented in Fitzmaurice *et al* (1977). The parameters give, for the particular orientation, the lidar cross-section and number of corner cubes, in rows, contributing to the strength of returning signal. Also given is the optical distance of each row of reflectors from the spacecraft centre of gravity. We use the effective cross section of the cubes in their rings, of known distances from the centre of the satellite, to carry out a convolution of our system signature with that of Lageos. In this estimate of the shape of the returning pulse we ignore the effects of changing polarisation, which mainly affects the amplitude of the convolved pulse, and not its shape (Fitzmaurice *et al* 1977.) To model the return signatures from Ajisai we use the results of a computer simulation carried out by Sasaki and Hashimoto (1987). They find that the number of retroreflector sets contributing to the return signal from a given single laser pulse can only be 1, 2 or 3.5, and give the computed pulse shape in each of these 3 cases. The laser used in their simulation is gaussian in profile, of standard deviation 33 ps. From the published profiles, we can infer the spread distributions, consisting of lidar cross-sections and distances from spacecraft centre of gravity. We now have the information required to carry out a convolution with our system signature, in the same way as for Lageos. We assume that the rapid spin rate of Ajisai, of 40 rpm (Sasaki and Hashimoto, 1987) will ensure that for every pass all 3 possible orientations of the satellite will be sampled. We thus convolve our system signature with each of the spread distributions, and sum the resulting 3 distributions.

The results of the simulations for Lageos and Ajisai are shown in histogram form in Figures 3(a) and (b), where the quoted standard deviations are those of the fitted Gaussian distributions, also shown on the plots. For completeness we also present in Figure 3 the result of convolving our system separately with each of the 3 orientations of Ajisai.

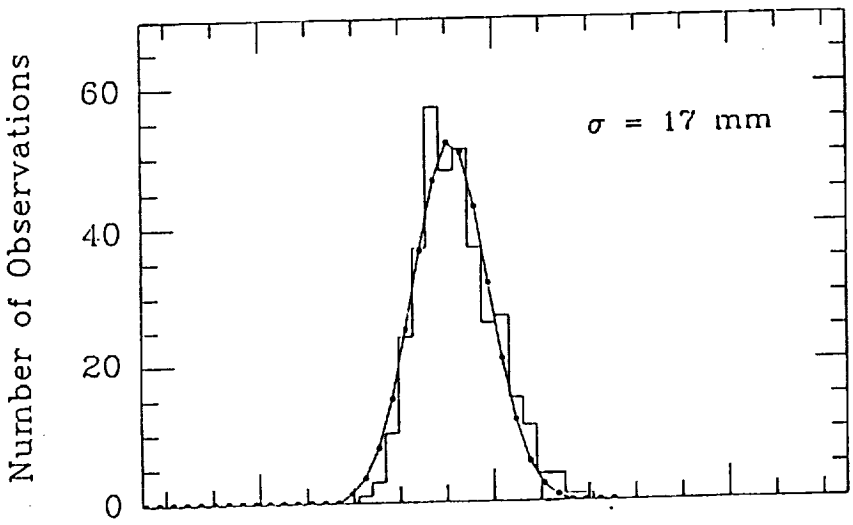


Figure 3. (a) Simulated Lageos range residual distributions.

of the SPAD detector is essential to avoid possible effects of non-uniformity within the chip. Resolution of this problem awaits further experimentation.

## 3. Satellite Signature Models.

We now take as our standard, single-photon system-signature the calibration distribution shown in Figure 1, and develop from it models of expected satellite return signatures, by convolution with the spread functions of Lageos and Ajisai. For Lageos, we take the model of cross-section parameters based upon row-by-row far-field diffraction pattern tests in polar orientation, presented in Fitzmaurice *et al* (1977). The parameters give, for the particular orientation, the lidar cross-section and number of corner cubes, in rows, contributing to the strength of returning signal. Also given is the optical distance of each row of reflectors from the spacecraft centre of gravity. We use the effective cross section of the cubes in their rings, of known distances from the centre of the satellite, to carry out a convolution of our system signature with that of Lageos. In this estimate of the shape of the returning pulse we ignore the effects of changing polarisation, which mainly affects the amplitude of the convolved pulse, and not its shape (Fitzmaurice *et al* 1977.) To model the return signatures from Ajisai we use the results of a computer simulation carried out by Sasaki and Hashimoto (1987). They find that the number of retroreflector sets contributing to the return signal from a given single laser pulse can only be 1, 2 or 3.5, and give the computed pulse shape in each of these 3 cases. The laser used in their simulation is gaussian in profile, of standard deviation 33 ps. From the published profiles, we can infer the spread distributions, consisting of lidar cross-sections and distances from spacecraft centre of gravity. We now have the information required to carry out a convolution with our system signature, in the same way as for Lageos. We assume that the rapid spin rate of Ajisai, of 40 rpm (Sasaki and Hashimoto, 1987) will ensure that for every pass all 3 possible orientations of the satellite will be sampled. We thus convolve our system signature with each of the spread distributions, and sum the resulting 3 distributions.

The results of the simulations for Lageos and Ajisai are shown in histogram form in Figures 3(a) and (b), where the quoted standard deviations are those of the fitted Gaussian distributions, also shown on the plots. For completeness we also present in Figure 3 the result of convolving our system separately with each of the 3 orientations of Ajisai.

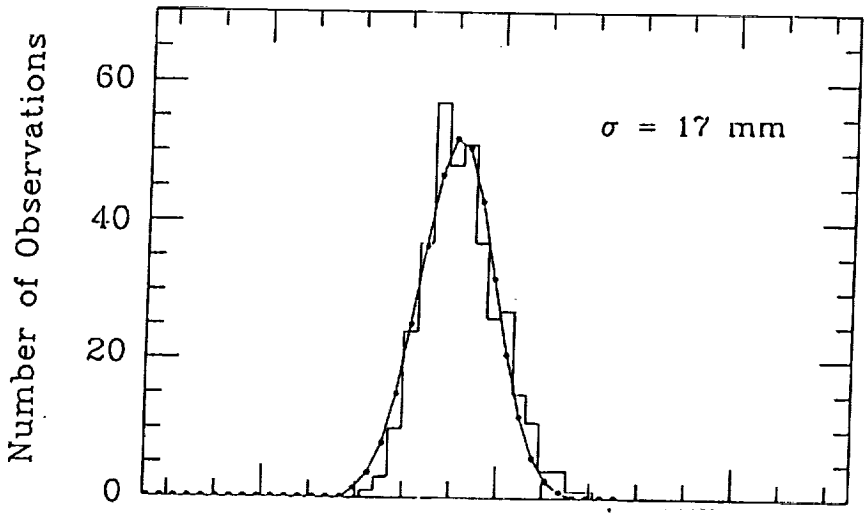


Figure 3. (a) Simulated Lageos range residual distribution

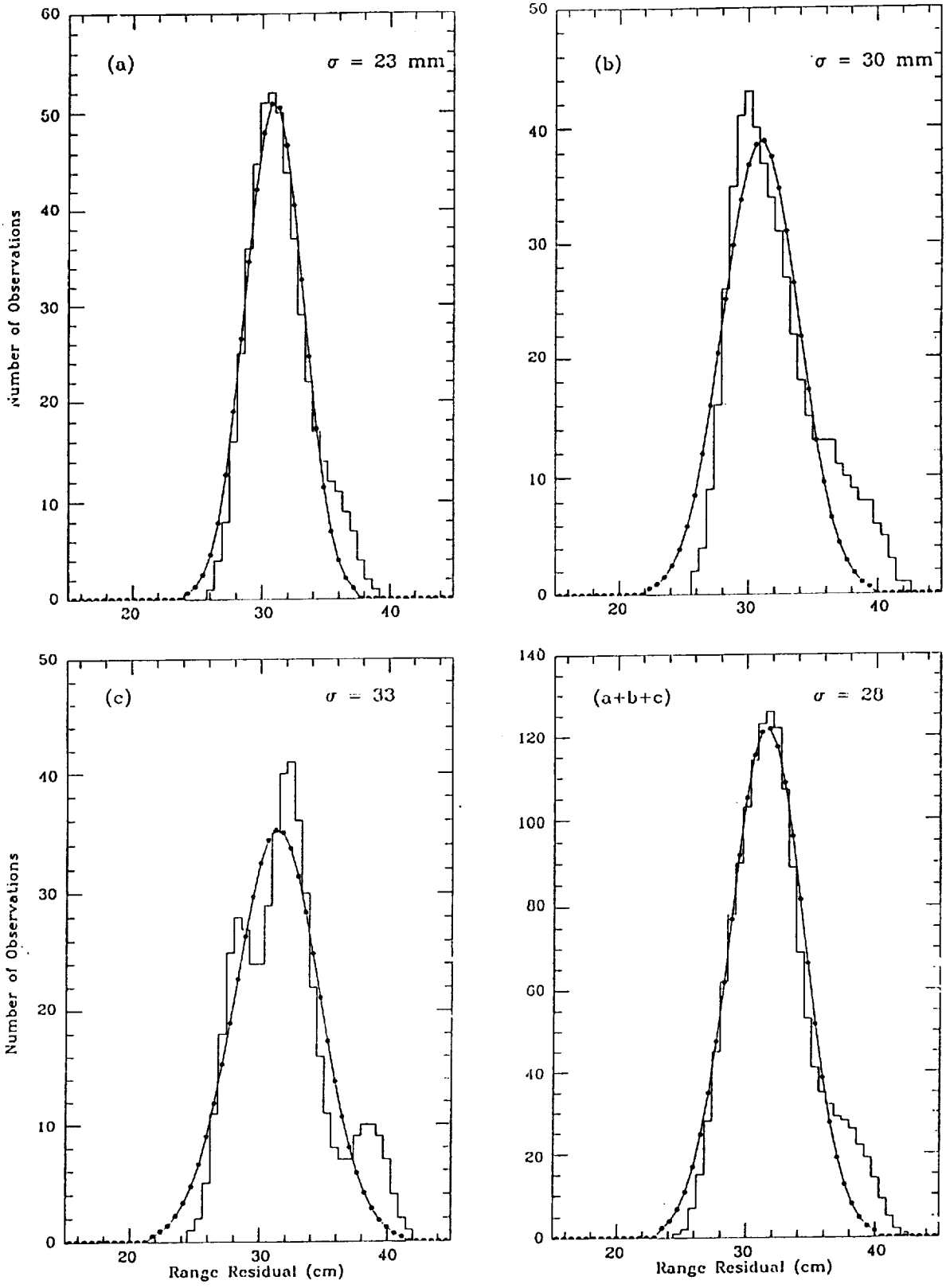


Figure 3. (b) Simulated Ajisai range residual distributions.

### 3.1 Discussion.

The standard deviation of the simulated Lageos data (1.7 cm) is close to our observational mean of 1.8 cm, and the appearance of the simulated and observed histograms is similar. The underestimate of the observed scatter by our model may be attributed to various causes; neglect of atmospheric turbulence (Gardner, 1976); neglect of coherency fading induced by the satellite, and the single satellite orientation chosen for the model. The models of the Ajisai return signatures give standard deviations of between 2.3 and 3.3 cm, which compare well with the observational results. There is some evidence in the Ajisai observations of variations of signature with pass circumstances, which may be due to the dominance of a particular satellite orientation or orientations for a given ground track.

## 4. Multi-photon Returns.

The foregoing discussion is based upon return energies at the single photon level; the detected photon is considered to be a random event taken from a population formed by the convolution of the laser pulse distribution with that of the satellite response. We now consider the effects of a larger number of photons reaching the single-photon detector, in order to quantify the subsequent systematic effects caused by a signal-strength-dependent variation of the mean reflection distance to the satellite.

### 4.1 Observations and reduction.

Experiments were carried out using Ajisai since it is relatively easy to obtain a large variation in received energy from the large target. The variation from single photon to multiple photon levels was achieved during the experimental passes by altering the divergence of the laser beam and hence the energy density at the satellite. The observations were filtered in the standard way, by using them to solve for corrections to the predicted orbit. However, it was found that this process did not remove all trends from the range residuals, indicating the presence of systematic range biases which varied during the passes. We found that it was necessary to divide each pass into a number (6) of segments, and use the processing software to filter the observations in each segment separately. The resulting scatter plot for one of the experimental passes is shown in Figure 4. The residuals from each of the six segments are shown in histogram form in Figure 5, along with the standard deviations of the fitted Gaussian distributions.

We calculate the average percentage return rates at intervals of 30 seconds throughout the passes by counting the numbers of satellite returns and the numbers of pre-return noise detections. Given that the laser fires 10 shots per second, the true percentage return rate in each 30-second interval is then

(number of true range measurements*100)/(30*10 - number of noise events)

On the assumption that the quantum efficiency of the SPAD is 20%, we calculate from these corrected return rates the average numbers of photons in each return. However we found that in several of the 30-second intervals the calculated return rate was nearly 100%. At such return levels we cannot reliably estimate the mean number of returning photons, which may be far in excess of the 16 estimated for a near 100% rate. Where possible, we have used these 30-second mean values to estimate the mean numbers of photons contributing to the observations in our 6 segments, and these averages are shown in Figure 5. For those 2

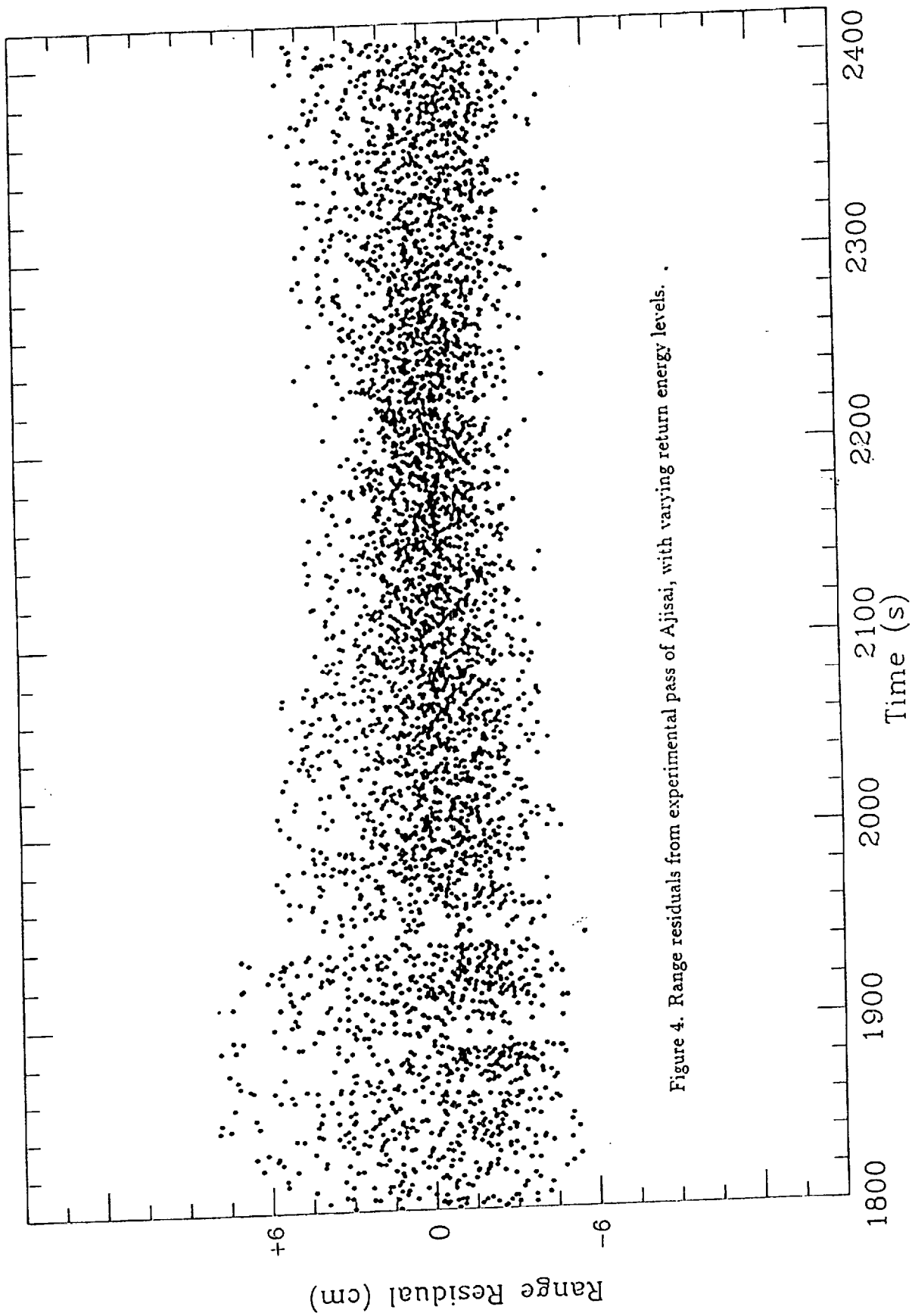


Figure 4. Range residuals from experimental pass of Ajisai, with varying return energy levels.

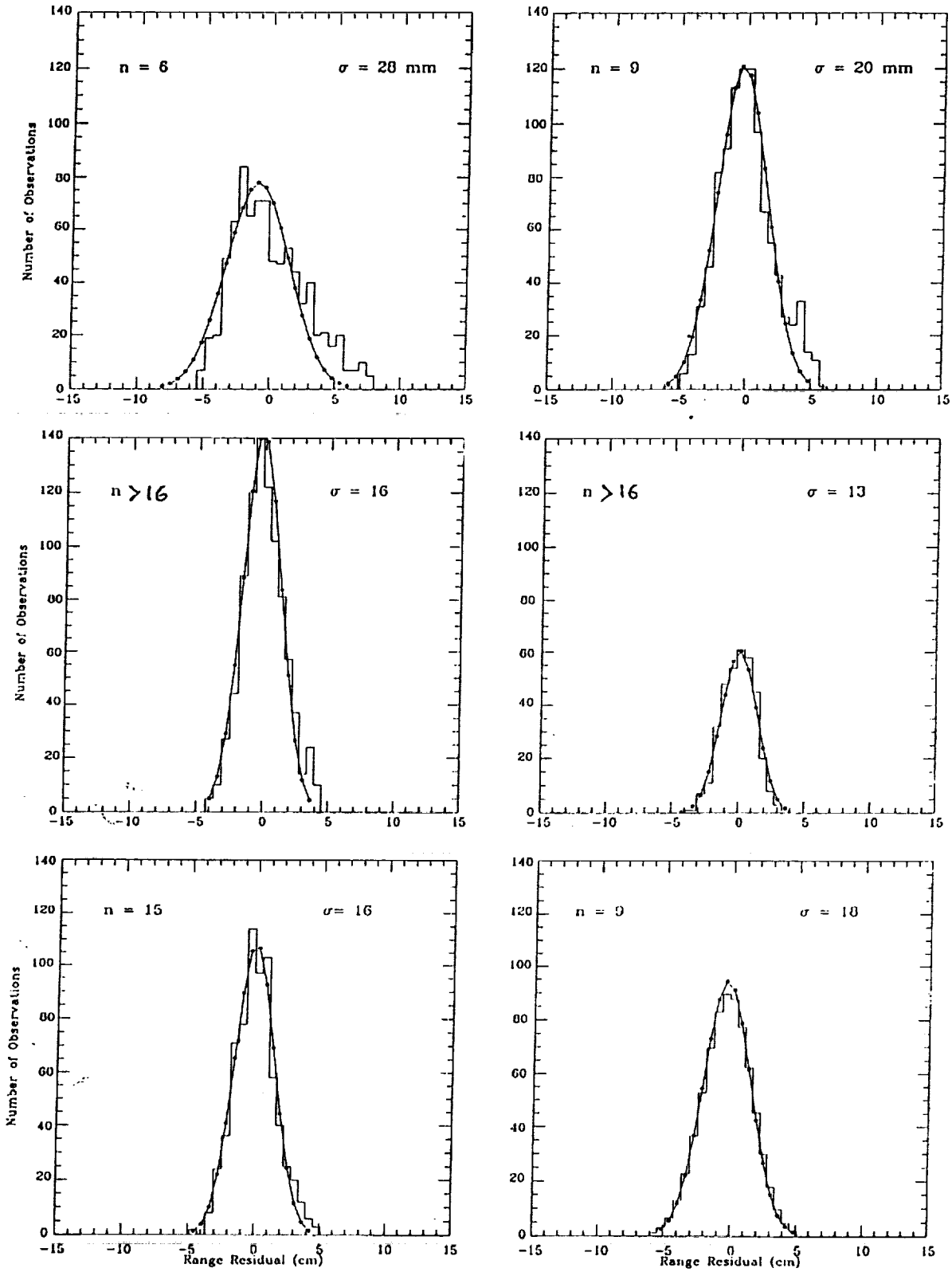


Figure 5. Distribution of range residuals from Ajisai pass as a function of average numbers $n$ of returning photons.

segments where the average return rates were near 100%, we have asigned the numbers of photons as >16, but remark that the true numbers could be several times as large.

### 4.2 Model and Discussion.

There is a clear variation of histogram shape and single-shot precision with change of signal strength. At low return rates equivalent to single photon returns, the distribution of residuals is similar to the 'standard' Ajisai distribution (Figure 1). For the high return rates little of the satellite signature remains in the distributions, and the histograms qualitatively and quantitatively resemble those from Starlette or ERS-1 (Figure 1).

These results cannot be used to detect a systematic variation of satellite mean reflection distance during the passes, because the method of reducing the observations absorbs any such corrections. However we can use models to predict both the increase of precision and this change of mean reflection distance as a function of numbers of photons in each return. We model the time-distribution of the returning photons, from which we may sample a variable number, by convolution of the Ajisai spread distributions with a Gaussian distribution of FWHM 50 ps, to represent the laser. To model the effect of $n$ photons reaching the detector, we use a random number generator to pick one 'photon' from our time-distribution of photons, then record its time-location within the distribution, and repeat the process $n$ times. We then sort this sequence of $n$ relative event times into chronological order of arrival at the detector. We model the 20% efficiency of the detector by stepping through the $n$ events in time order, at each step generating an integer random number in the range 1-5. If the random number is 1, the event is accepted (detected). If the random number is not 1, the next event is 'tested'. In this way we generate a large number of event times each resulting from the selection of a single photon from a series of returns containing an average of $n$ photons. The mean and standard deviation of these event times are computed and converted to range in cm. The standard deviation values are added quadratically to the estimated system jitter (0.8 cm) to fully model the observations. The results of simulations of range precision and biases from Ajisai for values of $n$ between 1 and 50 are shown in Figures 6a and 6b, where the results have been joined by continuous lines. The 30-second average observed values of precision, where they can be reliably estimated (see section 4.1) from our experimental Ajisai passes, are shown as dots on the graph and agree well with those predicted. The predicted range bias curve in Figure 6b expresses the expected change of mean reflection distance from the satellite centre of mass as a result of increasing the number of photons reaching the detector in each laser return. Most of the bias, which contains a contribution from the finite pulse length of the laser (FWHM 50ps), is seen to take effect between signal strengths at the single photon level up to an average of about 40 photons per return. Little change is predicted with increasing numbers of photons beyond that point.

### 4.3 Lageos Centre-of-mass correction.

We can use the above techniques to estimate the magnitude of a systematic range-bias for Lageos, in the context of worldwide SLR systems working at different return-signal levels. Figure 6 shows the results of a computation of the range bias as a function of average number of photons reaching the detector, for 2 modelled laser pulse-lengths. The magnitude of the change of the effective reflection distance from the satellite centre of mass is about 1.3 cm for a variation of return level from single-photons to the 40 photon level. This result

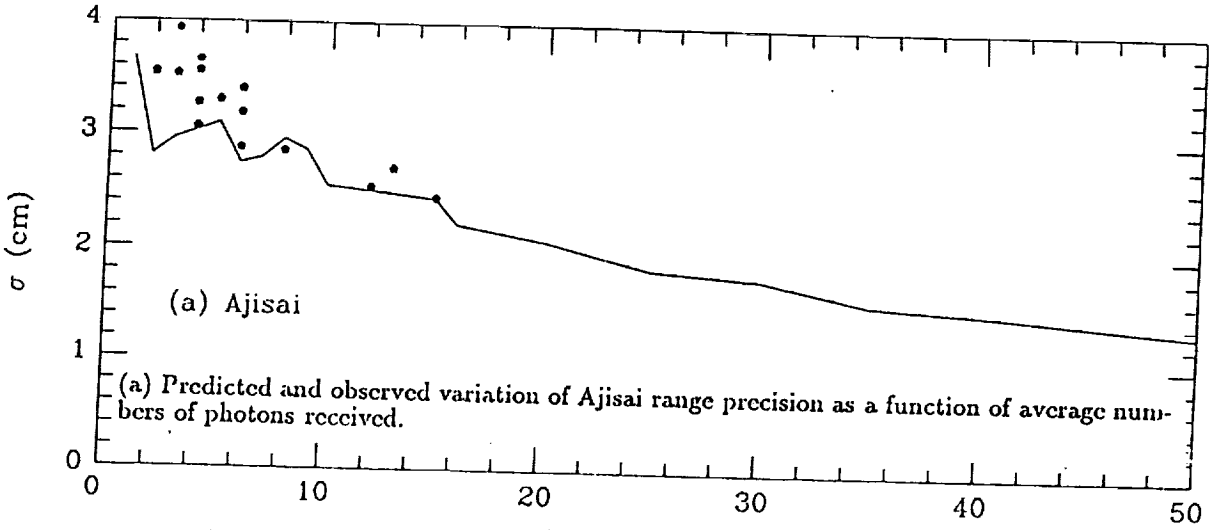


(a) Predicted and observed variation of Ajisai range precision as a function of average numbers of photons received.

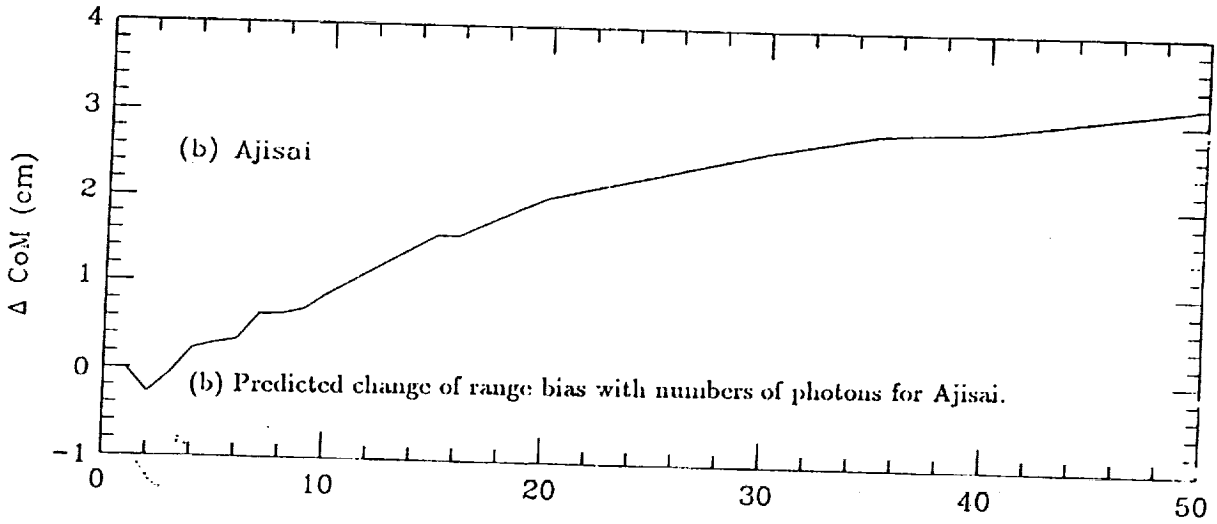


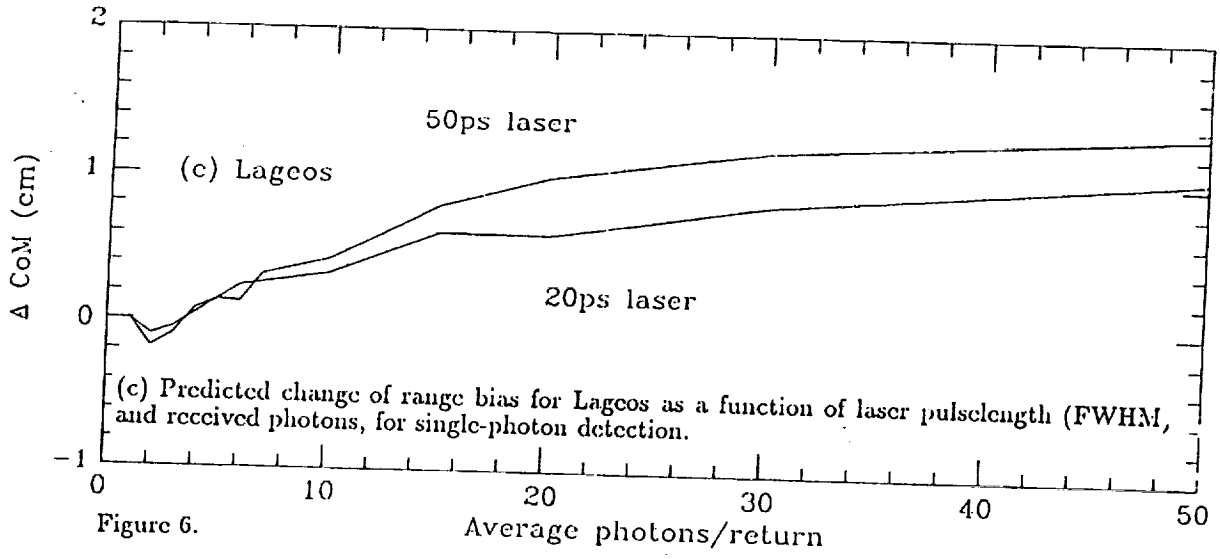


Figure 6.

implies that an SLR system receiving and detecting single photons, and using a laser with a pulsewidth (FWHM) of 50 ps, is on average effectively observing a distance 1.3 cm closer to the satellite centre of mass than a single-photon detection system receiving more than about 40 photons per shot. Removing from this figure the effect of the length (FWHM) of the laser pulse, the satellite-induced range bias amounts to about 0.6 cm. The recommended centre-of-mass correction for Lageos is 25.1 cm for leading-edge, half-maximum detection of a large return pulse, and 24.9 for peak detection (Fitzmaurice *et al*, 1977). We assume that the electronic detection of the peak of a large return pulse is equivalent, in terms of distance from cenre of mass, to the formation of the mean of a set of range residuals arising from the detection of single photons. For the Herstmonceux system working at the level of single photon returns, the appropriate centre-of-mass correction should therefore be the same as for the large-pulse, peak-detection systems, *ie* 24.9 cm. However, for single-photon systems departing from the single photon regime, the implications of this investigation are that the centre of mass correction should be *increased* from the 24.9 cm by an amount as given in Figure 6, depending upon the laser pulse-length and the number of photons reaching the detector.

## 5. Conclusion

Using observations from the UK single-photon SLR system, we have demonstrated that the observational scatter contains a satellite-dependent signature, and that this signature varies as expected with the number of photons reaching the detector. The implications of this variation upon the corrections required to relate range observations to the centres-of-mass of the satellites is modelled and discussed. The magnitude of the effect is system-dependent since it depends both on the number of photons reaching the detector, and hence on laser energy level and local atmospheric conditions, and upon the laser pulse length. A graph is presented giving a calculated, energy and pulse-length dependent, center of mass correction for Lageos range data obtained using single-photon detection, which varies by 1.3 cm over the range of the parameters considered.

## 6. Acknowledgements

All of the observations reported here were carried out by the SLR team at Herstmonceux, East Sussex, UK, under the direction of the station manager Dr. Roger Wood. The team's interest in carrying out the non-standard observations is appreciated. I thank Dr. Andrew Sinclair, Head of the RGO Space Geodesy Group, for his comments throughout the work on this project.

## 7. References

Fitzmaurice, M.W., P.O. Minott, J.B. Abshire and H.E. Rowe. 1977. *Nasa Technical Paper 1062.*

Gardner, C.S. 1976. Effects of random path fluctuations on the accuracy of laser ranging systems. *App. Optics, Vol 15, No. 10.*

Prochazka, I., K. Hamal and B. Sopko, 1990. Photodiode Based Detector Package for Centimeter Satellite Ranging, *Proc. 7th Int. Workshop on Laser Ranging Instrumentation, Matera, Italy, 1989.*

Sasaki, M and H. Hashimoto. 1987. Launch and Observational Programme of the Experimental Geodetic Satellite of Japan. *IEEE Trans. on Geoscience and Remote Sensing, Vol GE-25, No. 5.*